

# Effect of Filler Metal and Postwelding Heat Treatment on Mechanical Properties of Al-Zn-Mg Alloy Weldments

Y.E. Wu and Y.T. Wang

(Submitted December 17, 2009; in revised form February 26, 2010)

This study investigated the effect of three filler metals, namely ER5356, ER5183, and ER5556, and various postwelding heat treatments, including natural aging, artificial aging, T6 and T73, on mechanical properties of AA7005 and AA7003 alloys. Microhardness in the fusion zone, heat-affected zone, and base metal were measured. Both scanning electron microscopy and transmission electron microscopy analyses were also conducted. Results show that AA7005 and AA7003 welded with filler metal ER5356 achieved significant enhancement both in hardness and ultimate tension strength after postwelding heat treatments, indicating that ER5356 is the most suitable filler metal for welding Al-Zn-Mg alloys. While both T6 and T73 heat treatments can enhance precipitation hardening in the fusion zone, T73 yields a wider precipitation free zone on the grain boundary; thus making it a better approach to increasing fusion zone strength in weldments. In sum, appropriate choice of filler metal and heat treatment can enhance overall mechanical strength of welded alloys.

**Keywords** Al-Zn-Mg alloy, ER5183, ER5356, ER5556, mechanical property, postwelding heat treatment

## 1. Introduction

In recent years, industries have devoted much effort to the research and development of manufacturing aluminum (Al) alloys and its applications in the hope of conserving energy and reducing carbon dioxide emission, thus minimizing the negative impact on the environment. Al alloys of light-weight and high-specific strength have been developed and widely applied in bicycles and vessels as well as vehicle and aerospace industries.

Welding is often used in manufacturing of Al alloys. The strength of the fusion zone determines the usability and quality of weldments. Despite softening of the heat-affected zone (HAZ) due to welding, appropriate postwelding heat treatment can help restore the overall strength of weldments (Ref 1, 2). When a filler of high-magnesium (Mg) content (3 wt.%) is used (Ref 3), the HAZ of AA7003, though of low copper content (Cu < 0.1%), can restore 80-85% of base metal strength after natural aging (NA) or artificial aging (AA) (Ref 4).

ER5183, ER5556, and ER5356 are three common filler metals used in welding Al-Zn-Mg alloys. Among them, ER5183 and ER5556 have relatively higher manganese (Mn) content. Previous studies (Ref 5, 6) have pointed out the close relationship between the chemical composition of filler metal and the shape, size and distribution of precipitates from the

AA7000 series Al alloys after postwelding heat treatments. In view of this, Al-Zn-Mg alloys, namely AA7003-T5 and AA7005-T1 were used as base metal, and three high-magnesium filler metals of different compositions, namely ER5183, ER5556, and ER5356 were used in this study.

There are currently several approaches to welding. For example, metal inert gas (MIG) welding is mainly applied to thick plates exceeding 3 mm in thickness. It is suitable for large-scale mass manufacturing but the welding quality varies; hence, there is ongoing research on how to achieve uniform welding performance. On the other hand, friction stir welding (FSW) is widely employed in thin-plate welding without the need of filler metal. Although good mechanical properties of weldments can be obtained by this automated approach, the investment involved and the cost incurred are both extremely high. Tungsten inert gas (TIG) welding can enhance quality of weldments through the use of appropriate filler metal and postwelding heat treatment. The investment and cost required are comparatively lower than those of FSW. Hence, TIG possesses advantages of both MIG and FSW and more effort is needed for exploring its application to welding of Al alloys. In this study, all underwent TIG welding, followed by different postwelding heat treatments to explore the effect of filler composition on mechanical properties of alloy weldments and to optimize the welding process by determining the most suitable filler metal for Al-Zn-Mg alloys.

## 2. Experimental Procedure

### 2.1 Materials

The base materials used in this study are AA7005 and AA7003 alloys in the form of 6-mm thick plates and three filler metals recommended by the Welding Handbook (Ref 7), namely ER5183, ER5556, and ER5356. The chemical

Y.E. Wu and Y.T. Wang, Department of Mechanical Engineering, National Taiwan University of Science and Technology, 43 Keelung Rd., Sec. 4, Taipei 10607, Taiwan, R.O.C. Contact e-mails: albertwu@mail.ntust.edu.tw and tr754604@msa tra.gov.tw.

**Table 1 Chemical compositions (wt.%) of the AA7003 and AA7005 alloys**

Element	Zn	Mg	Mn	Fe	Cr	Si	Ti	Cu	Al
AA7003	6.42	0.77	0.20	0.17	0.09	0.13	0.02	0.05	Bal.
AA7005	4.43	1.26	0.36	0.10	0.10	0.07	0.02	0.01	Bal.

**Table 2 Chemical compositions (wt.%) of filler metals**

Element	Mn	Mg	Cr	Ti	Al
ER5183	1.03	5.07	0.05	0.04	Bal.
ER5556	0.71	4.77	0.16	0.10	Bal.
ER5356	0.13	4.56	0.06	0.02	Bal.

composition of the alloys and filler metals studied is shown in Table 1 and 2, respectively (Ref 8).

## 2.2 Welding Process

The specimen plates for welding are of size 100 mm ( $L$ )  $\times$  50 mm ( $W$ )  $\times$  6 mm ( $t$ ). TIG welding was performed on AA7005 with ER5183, ER5556, and ER5356, while AA7003 was welded only with ER5356, which is found to be a filler metal of better mechanical properties. The extrusion direction is vertical.

## 2.3 Postwelding Heat Treatment

Tables 3 and 4 describe the different postwelding heat treatments applied to AA7003 and AA7005, respectively. In order to examine the influence of heat treatment on the microstructure and properties of welded alloys, the weldments were subjected to one of the following heat treatments: (1) NA; (2) AA; (3) T6, which adopts production parameters for achieving strength of 372 MPa according to ASM (Ref 9); and (4) T73, which adopts heat-treatment parameters for manufacturing AA7075 with electrical conductivity of 40% IACS as specified by the Aluminum Association specification (Ref 10). Solid solution treatment and artificial aging involves putting the alloys into salt-bath furnace and oil-bath furnace, respectively. Temperature was controlled within  $\pm 2$  °C of the experimental parameter. The quenching liquid is 5% saline at room temperature.

## 2.4 Tests on Microhardness

The thermal cycle of welding causes great changes in the strength of the fusion zone and base metal; and there exists an almost linear relationship between strength and microhardness. Hence, measuring the changes in microhardness of the fusion zone and base metal can shed light on the effect of welding.

Hardness measurements of welded specimens were carried out using a Vickers hardness machine applying a load of 300 gf for 15 s.

To study the microhardness of the welded specimens, tests were conducted on the cross section of the alloy weldments at interval of 0.6 mm with  $\sigma$  (standard deviation) equal to  $\pm 2$  HV.

## 2.5 Tensile Test

Standard tensile tests were performed on the specimens with the weld seam positioned transversely across the middle of the

**Table 3 Experimental parameters of postwelding heat treatments applied to AA7003 weldments**

Temper	Heat treatment parameter
AA	Only performing 120 °C/42 h condition in oil-bath furnace
T6	Solid solution 470 °C/40 min + water quenching + 80 °C/14 h + 120 °C/42 h
T73	Solid solution 470 °C/40 min + water quenching + 80 °C/14 h + 107 °C/8 h + 168 °C/7 h

AA, Artificial aging

**Table 4 Experimental parameters of postwelding heat treatments applied to AA7005 weldments**

Temper	Heat treatment parameter
NA	Only performing 18-day-natural-aging at room temperature
T6	Solid solution 470 °C/40 min + water quenching + 80 °C/72 h + 120 °C/72 h
T73	Solid solution 470 °C/40 min + water quenching + 80 °C/72 h + 107 °C/8 h + 168 °C/17 h

NA, Natural aging

weldments. The final results of the tensile test are the average of three measurements.

## 2.6 SEM Analysis

The diffusion of alloy elements between the fusion zone and base metal was examined under a scanning electron microscope (SEM) with an electron dispersive x-ray spectrometer (EDS).

## 2.7 TEM Microstructural Analysis

After grinding and polishing, the specimens were made into thin foils by jet thinning and etched in a solution containing nitric acid and methanol at a volume ratio of 1:4. The microstructure was examined under a transmission electron microscope (TEM) operated at 15 kV. An ion miller was also employed to increase the area of the thin-foil specimens.

# 3. Results and Discussion

## 3.1 Effects of Postwelding Heat Treatments on Hardness of Al-Zn-Mg Alloys

Figure 1 shows the cross section microhardness profile of AA7005/ER5183, AA7005/ER5556, AA7005/ER5356, and

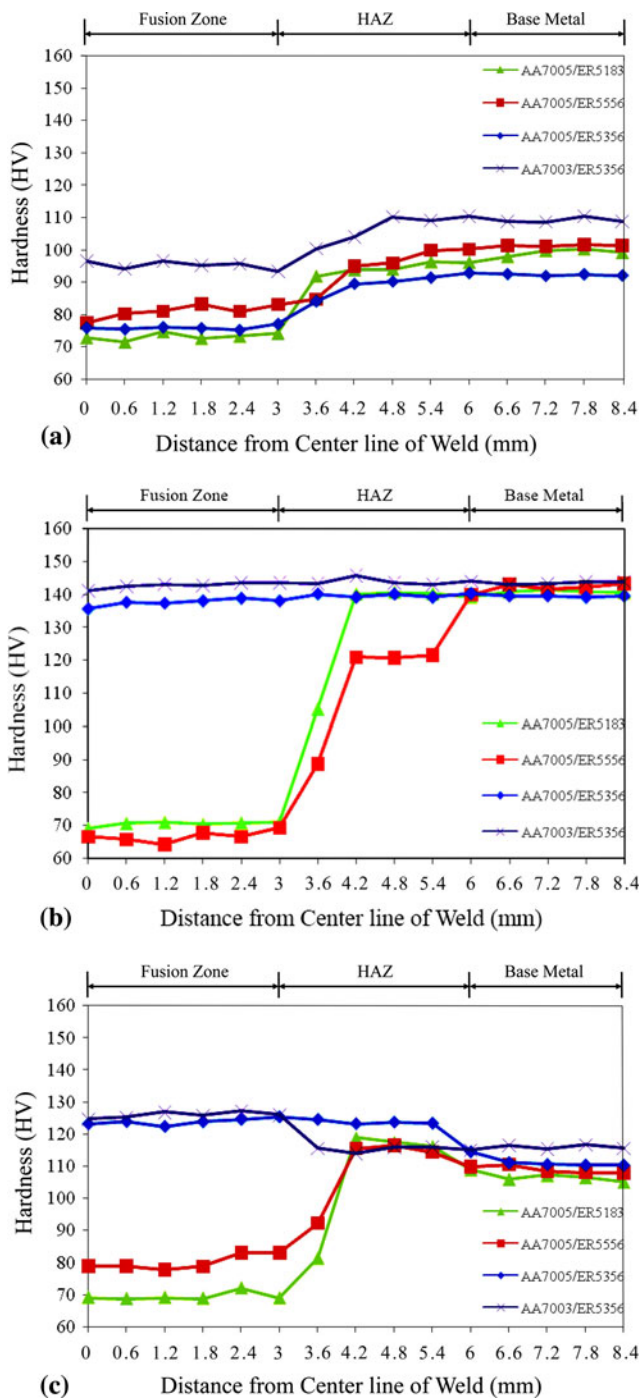


**Fig. 1** Cross section microhardness profiles of (a) as-welded Al-Zn-Mg alloys, (b) T6-treated Al-Zn-Mg alloys, and (c) T73-treated Al-Zn-Mg alloys

AA7003/ER5356 weldments after undergoing different postwelding heat treatments. As seen in the results of as weldments shown in Fig. 1(a), only slight difference in microhardness is observed, with the base metal having greater microhardness than the fusion zone and HAZ. Among the different alloy weldments, AA7003/ER5356 weldments show the highest microhardness in the fusion zone (95 HV) and base metal (105 HV), indicating that AA7003 alloy with high Zn/Mg content (8.34) has greater strength than AA7005 with low Zn/Mg content (3.52). In the absence of postwelding heat

treatments, most of the Zn and Mg atoms solidified in the fusion zone tend to form different intermetallic compounds. The few Zn and Mg atoms solidified in the Al base matrix cannot achieve precipitation hardening effect through aging heat treatment.

Figure 1(b) displays the cross section microhardness profiles of various alloys after postwelding T6 heat treatment. As can be seen, for both AA7005/ER5356 and AA7003/ER5356, the microhardness in the fusion zone and HAZ rose to a level (130-140 HV) similar to that of the base metal. Compared with the results of the as weldments shown in Fig. 1(a), the increase in microhardness in the fusion zone, HAZ and base metal achieved by T6 was significant. On the other hand, the fusion zone for both AA7005/ER5183 and AA7005/ER5556 showed no enhancement in microhardness. A sharp increase in microhardness of the HAZ and a marked difference in microhardness between the fusion zone and base metal were observed, indicating that postwelding T6 heat treatment can help enhance microhardness in the base metal for both AA7005 and AA7003 as well as microhardness in the fusion zone when welded with ER5356.

Figure 1(c) shows the cross section microhardness profiles of various alloys after postwelding T73 heat treatment. As seen in Fig. 1(c), for both AA7005/ER5356 and AA7003/ER5356, the microhardness in the fusion zone rose to 125 HV, which was higher than that of the base metal (115 HV). In other words, AA7005/ER5356 and AA7003/ER5356 are high-quality weldments with good fusion zone hardness. Compared with the results of the as weldments shown in Fig. 1(a), the increase in microhardness in the fusion zone, HAZ and base metal achieved by T73 was significant, though not as high as that achieved by T6. Such difference can be attributed to over-aging that causes decrease in microhardness. The same phenomenon has also been observed by Speidel (Ref 10), who found a reduction in microhardness of the base metal due to over-aging that occurred in the two-stage artificial aging. Microhardness of the fusion zone both for AA7005/ER5183 and AA7005/ER5556 after T73 heat treatment was 70-80 HV, the same range as that for as-welded and T6-treated alloys, as seen in Fig. 1(a) and (b), respectively. This reveals that heat treatment failed to enhance microhardness in these weldments. In addition, similar to T6-treated alloys, a sharp increase in microhardness was also seen in the HAZ of T73-treated AA7005/ER5183 and AA7005/ER5556.

As-welded Al-Zn-Mg alloys show relatively lower microhardness due to melting of precipitates under the thermal cycle of high-temperature welding (Ref 11), which causes reduction in microhardness of the fusion zone and HAZ. Both ER5183 and ER5556 are high-magnesium filler metals, with precipitates of  $MnAl_6$ ,  $(MgMn)_3Al_{10}$ , and  $Mg_5Al_8$  easily formed inside the grain matrix after high-temperature welding. Previous research by Embury and Nicholson (Ref 12) has found that these precipitates will melt at 500 °C. In this study, the solid solution treatment was conducted at 470 °C, at which  $MnAl_6$  could not be melted again into the matrix, thus hampering the diffusion of elements in the base metal. This would in turn undermine the mechanical properties of the alloy weldments. Despite undergoing different postwelding heat treatments, AA7005/ER5183 and AA7005/ER5556 showed no improvement in strength, indicating that ER5183 and ER5556 are filler metals not responsive to heat treatment.

On the contrary, ER5356 showed good response to postwelding T6 and T73 heat treatments, which led to significant increase in microhardness. This evidences that precipitates from

filler metal of high Mg and low Mn proportion can enhance the strength of Al-Zn-Mg alloys.

### 3.2 Effects of Postwelding Heat Treatments on Strength of Al-Zn-Mg Alloys

Results of tensile tests for weldments made with ER5356 are listed in Table 5. All tensile specimens broke in the fusion zone adjacent to the fusion boundary except the one subjected to T73 treatment. This shows that fusion zone strength of T73-treated weldments was enhanced by the heat treatment. As a result, cracks occurred in the HAZ and base metal only, indicating superior welding performance. In addition, as seen in Table 5, the ultimate tension strength (UTS) of both AA7003 and AA7005 after T6 heat treatment was the highest.

Figure 2 shows the relationship between UTS and hardness of AA7005 after AA at 120 °C with the specified T6 strength requirement indicated. As can be seen, there exists a linear relationship between the two for hardness above 50 HV. In view of the complicated and time-consuming procedure involved in preparing specimens for the tensile strength test, taking the hardness value as an indicator and reference of tension strength is a compromising solution which offers both efficiency and accuracy.

### 3.3 Effects of Element Diffusion on Mechanical Properties

**3.3.1 AA7005 Welded with ER5356, ER5183, and ER5556.** Figures 3-5 display the elemental analysis results of AA7005/ER5183, ER5556, and ER5356, respectively, after

**Table 5 Results of tensile tests for weldments welded with ER5356 filler metal**

Temper	Weldment	UTS, MPa	Fracture position
As-welded	AA7005	221	Fusion zone
	AA7003	257	Fusion zone
T6	AA7005	326	Fusion zone
	AA7003	335	Fusion zone
T73	AA7005	312	HAZ and base metal
	AA7003	308	HAZ and base metal

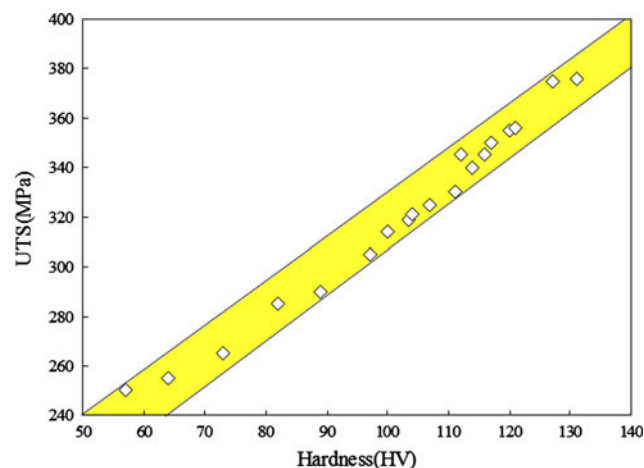
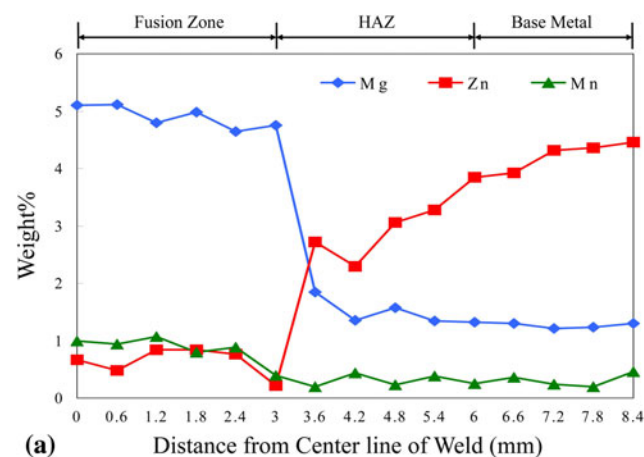


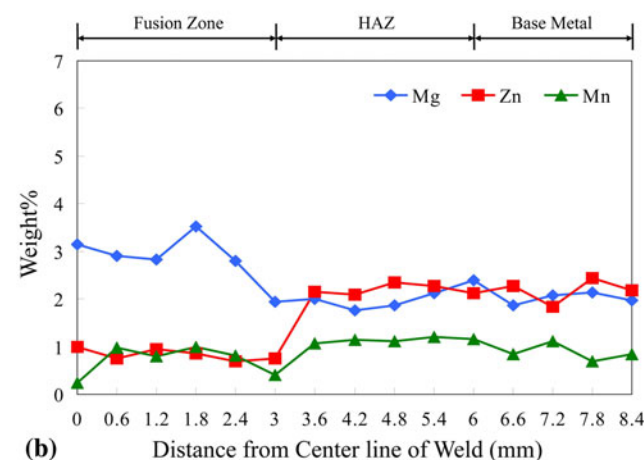
**Fig. 2** Relationship between hardness and ultimate tensile strength of AA7005 after AA at 120 °C

NA and T6 heat treatments, with wt.% of Mg, Zn, and Mn in the fusion zone and base metal shown. As seen in Fig. 3(a), there is significant difference in wt.% between Mg and Zn at 3 mm from the center line of the fusion zone, indicating poor diffusion between Mg and Zn, which forms an element clustering layer in AA7005/ER5183 after NA treatment. However, such element clustering phenomenon decreased gradually after T6 heat treatment as seen in Fig. 3(b). Poor element diffusion undermines the effect of precipitation hardening, which in turn reduces the microhardness of fusion zone. Similar findings were obtained for AA7005/ER5556 as shown in Fig. 4.

Comparatively, the element clustering layer between fusion zone and base metal for AA7005/ER5183 after NA, as seen in Fig. 3(a), is narrower than that for AA7005/ER5356 shown in Fig. 5(a). As seen in Fig. 5(b), the element clustering layer reduced progressively after postwelding T6 heat treatment. The complete solid solution treatment followed by quenching and aging enhances diffusion of element, thus producing even distribution of Mg and Zn between the fusion zone and base metal. This facilitates the precipitation of the hardened  $\eta$ -phase ( $MgZn_2$ ), which in turn enhances the strength of weldments. Such result is in agreement with the observation in Fig. 1(b), showing effective increase in microhardness in both fusion zone and base metal by T6 heat treatment.



**(a)** Distance from Center line of Weld (mm)



**(b)** Distance from Center line of Weld (mm)

**Fig. 3** Wt.% of elements in AA7005/ER5183 (a) after NA heat treatment and (b) after T6 heat treatment

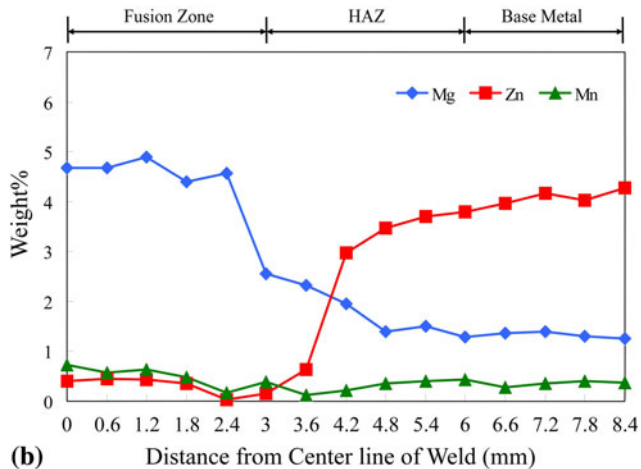
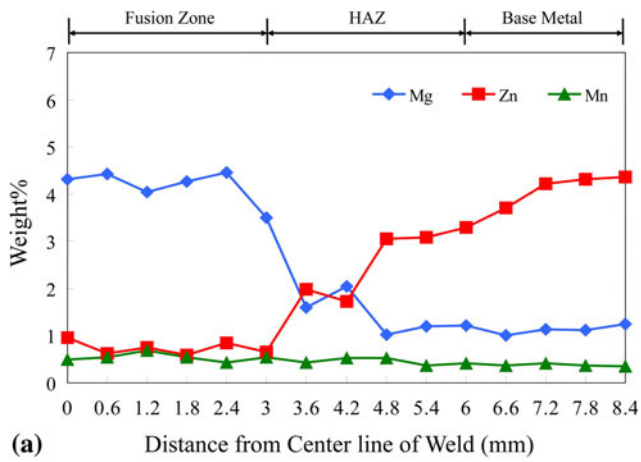


**Fig. 4** Wt.% of elements in AA7005/ER5556 (a) after NA heat treatment and (b) after T6 heat treatment

In sum, solid solution treatment can remove the element clustering layer and thus increase microhardness of AA7005/ER5356. However, solid solution treatment applied to AA7005/ER5138 and AA7005/ER5556 cannot narrow much the element clustering layer; thus affecting its effectiveness in weld strength enhancement.

**3.3.2 AA7003 Welded with ER5356.** Figure 6(a)-(c) displays the elemental analysis results of as-welded and heat-treated AA7003/ER5356, which show the wt.% of Zn, Mg, and Mn in the alloy weldment, respectively. As can be seen, there is wide variation in wt.% of elements in as-welded AA7003/ER5356. This is attributed to the effect of TIG welding segregation, which results in localized concentration of elements. In this study, the dilution ratio of the fusion zone calculated using the equation proposed by Metzger (Ref 13) is 66.8%, indicating segregation effect. Moreover, Metzger (Ref 13) also pointed out the positive correlation between dilution ratio of fusion zone and strength of weldments; that is, the higher the dilution ratio, the better the precipitation hardening effect will be. Hence, optimization of the postwelding heat-treatment parameters can compensate and enhance the mechanical properties of Al-Zn-Mg alloy weldments.

In the fusion zone, the alloying elements, which form precipitates during aging, were redistributed in the dendritic structure during solidification (Ref 4). Appropriate heat

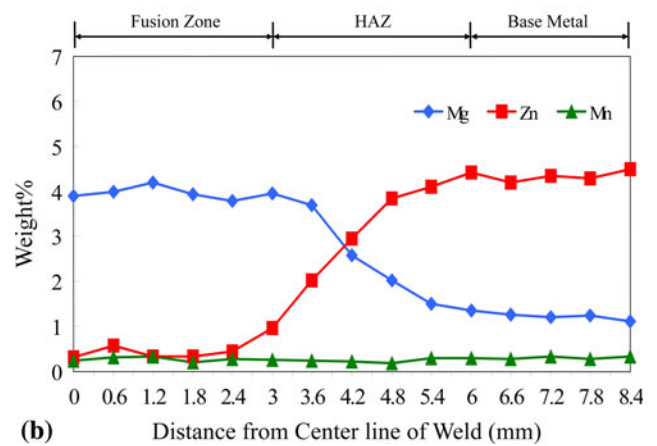
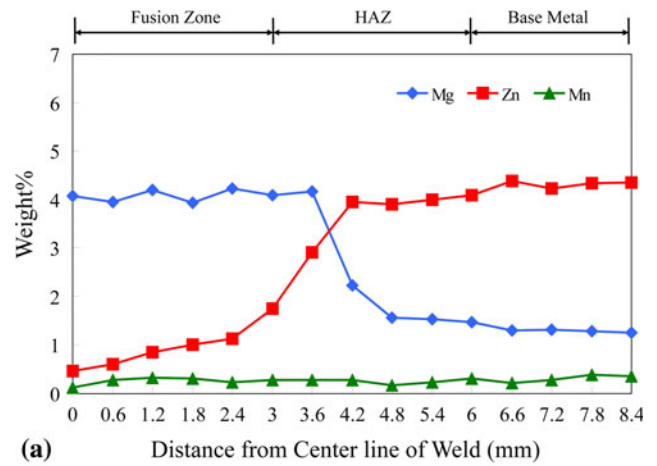


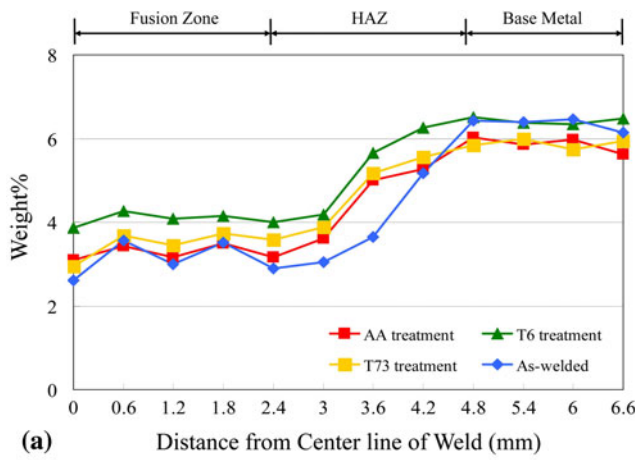
**Fig. 5** (a) Wt.% of elements in AA7005/ER5356 (a) after NA heat treatment and (b) after T6 heat treatment

treatment process can ameliorate welding segregation in the fusion zone, causing the changes in microhardness to become less marked. As seen in Fig. 6, the wt.% of elements in AA7003/ER5356 after AA heat treatment became less varied as a result of element redistribution. This indicates that AA heat treatment can help reduce the difference in precipitation hardening between the fusion zone and base metal. Note that in Fig. 6(b), there are marked changes in Mg distribution within the interval of 2.4-4.8 mm after postwelding T73 heat treatment, which affects the strength of the HAZ. Apart from this, even distribution of elements is seen in the fusion zone and base metal, which is attributed to the diffusion of elements promoted by solid solution treatment.

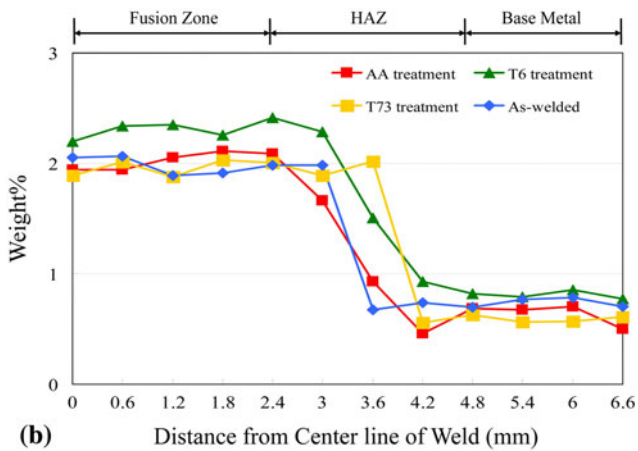
In sum, solid solution treatment can foster even distribution of different dissolved elements and facilitate the diffusion of Zn from the base metal into the fusion zone, thus enhancing precipitation hardening. The trend in element diffusion in heat-treated weldment can shed light on the effect of different heat treatments on strength of weldments.

### 3.4 Microstructure Observations of Fusion Zone Under TEM

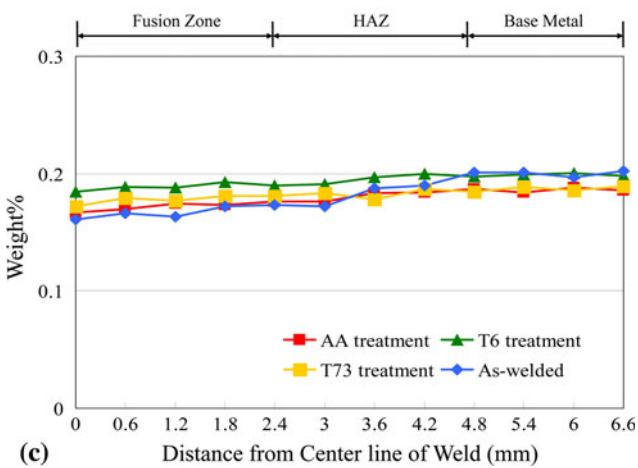
**3.4.1 AA7005 Welded with ER5356, ER5183, and ER5556.** Figure 7 displays the TEM image of AA7005/ER5356 fusion zone after T6 heat treatment. As can be seen, a dense hardened  $\eta'$ -phase is formed at the fusion zone matrix,



(a) Distance from Center line of Weld (mm)



(b) Distance from Center line of Weld (mm)



(c) Distance from Center line of Weld (mm)

**Fig. 6** Cross section microhardness profiles of (a) Zn, (b) Mg, and (c) Mn in as-welded and heat treatment AA7003 alloys

indicating precipitation hardening effect, which is not observed in AA7005/ER5183 fusion zone. Previous studies (Ref 11, 14, 15) pointed out that during solid solution treatment, the critical vacancy concentration in the matrix causes nucleation of precipitates in the Guinier-Preston (GP) zones. On the other hand, because of less variation in concentration of dissolved elements along the grain boundary, the vacancy concentration does not reach the critical level for nucleation of precipitates in GP zones. Hence, during quenching, the relatively

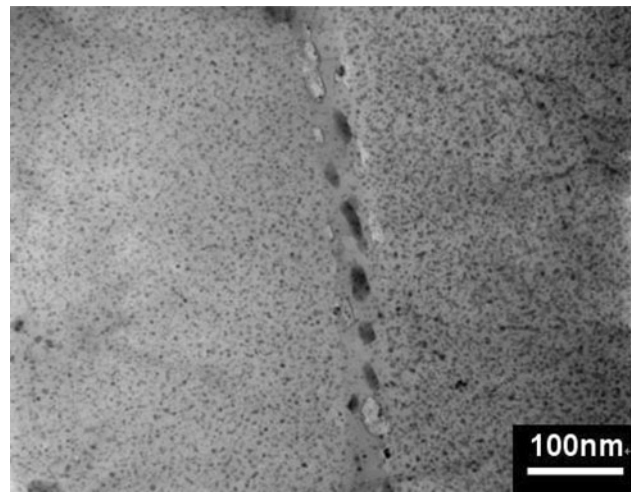


**Fig. 7** TEM image of AA7005/ER5356 fusion zone after T6 heat treatment

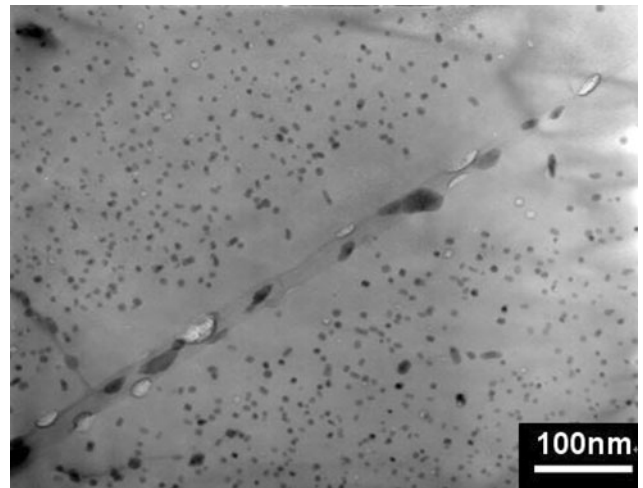


**Fig. 8** TEM image of AA7005/ER5356 fusion zone after T73 heat treatment

high-vacancy concentration in the matrix causes the dissolved elements at the grain boundary to diffuse toward the matrix, thus forming a precipitation free zone (PFZ).

Figure 8 displays the TEM image of AA7005/ER5356 fusion zone after T73 heat treatment. As can be seen, long aging duration results in growth of precipitates. Segments of large and coarse precipitates are found on the grain boundary and the PFZ becomes 100 nm wide.

In sum, solid solution treatment enhances element diffusion, thus achieving even distribution of Zn and Mg in weldments. This results in similar microstructure between the fusion zone and base metal in AA7005/ER5356. The enhancement in microhardness of the fusion zone varies according to the different aging treatments applied. The fusion zone of both AA7005/ER5183 and AA7005/ER5556 contains high wt.% of Mn. As a result, Al-Mn compounds are precipitated after solid solution and aging treatments. Yeomans (Ref 16) suggested using the stress-strain approach to improve the strength of both fusion zone and base metal in non-heat-treated Al alloy weldments of extremely low microhardness.

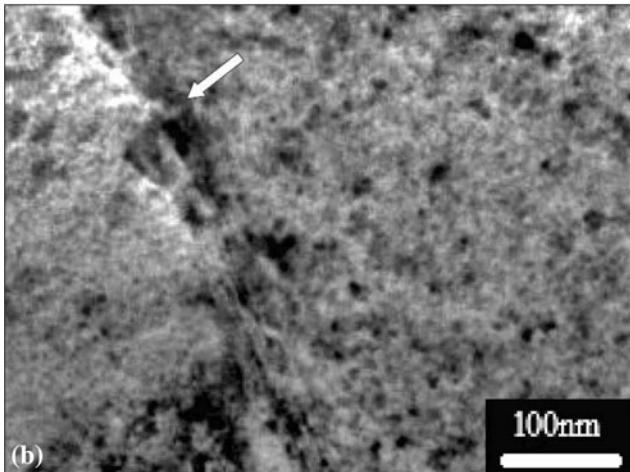
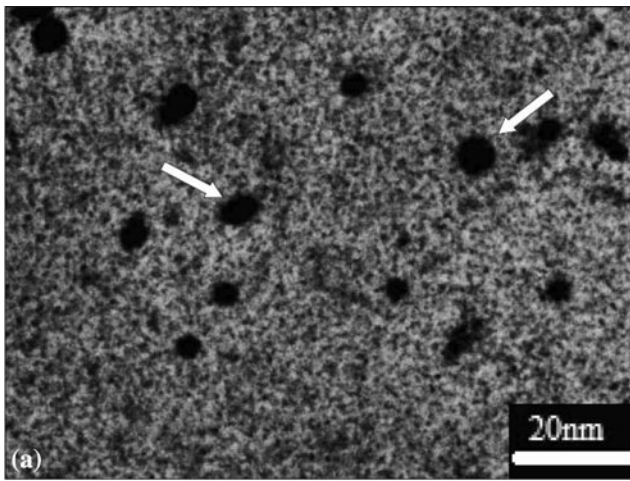
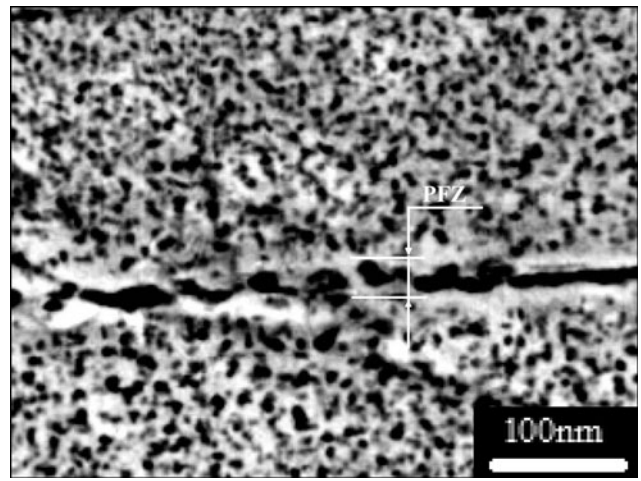


**Fig. 9** (a) TEM image of AA7005/ER5356 grain matrix after AA heat treatment. (b) TEM image of AA7005/ER5356 grain boundary after AA heat treatment

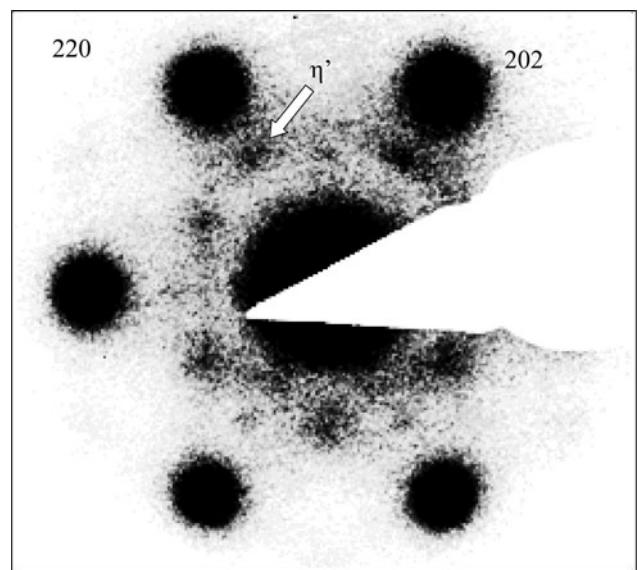
**3.4.2 AA7003 Welded with ER5356.** Figure 9 displays the TEM image of AA7003/ER5356 fusion zone after AA heat treatment. As seen in Fig. 9(a), the matrix of the fusion zone is filled with small dense precipitates, except for a few coarse precipitates indicated by arrows. The formation of these coarse precipitates is the result of incomplete solid solution of the dissolved elements. As for the grain boundary indicated by the arrow in Fig. 9(b), there exists no obvious PFZ on the two sides, which is attributed to the solid solution treatment.

Figure 10 displays the TEM image of AA7003/ER5356 fusion zone after T6 heat treatment. As can be seen, the matrix is filled with dense precipitates and there is a PFZ of 30 nm wide. Comparing Fig. 9(a) and 10 shows that precipitates formed after T6 heat treatment are denser and smaller, with no precipitation growth observed. The superior results obtained by T6 heat treatment compared with those by AA echo the finding of Thompson et al. (Ref 17), who reported the denser and smaller the precipitates, the better the precipitation hardening effect.

Figure 11 displays the selected area diffraction pattern (SADP) of AA7003/ER5356 after T6 heat treatment along the  $[111]_{Al}$  orientation. The stronger diffraction spots come from the Al base metal while the weaker diffraction spots are contributed by the precipitates. Our findings are in agreement



**Fig. 10** TEM image of AA7003/ER5356 fusion zone after T6 heat treatment



**Fig. 11** SADP of AA7003/ER5356 after T6 heat treatment along  $[111]_{Al}$  orientation

with the SADP of Al-Zn-Mg alloys after T6 heat treatment obtained by Werenskiold et al. (Ref 18). The  $\eta'$ -phase ( $MgZn_2$ ) is observed in both cases. The TEM image seen in Fig. 10, the SADP displayed in Fig. 11, and related studies (Ref 17, 18) in the literature all reveal that the presence of semi-integrated  $\eta'$ -phase after T6 heat treatment can improve the microhardness of the fusion zone.

Figure 12 displays the TEM image of AA7003/ER5356 fusion zone after T73 heat treatment. Comparing Fig. 10 and 12 shows that T73 heat treatment produces looser and larger precipitates in the matrix with a wider PFZ of 60 nm.

## 4. Conclusions

1. AA7003 and AA7005 welded with filler metal ER5356 achieved significant enhancement in hardness and UTS

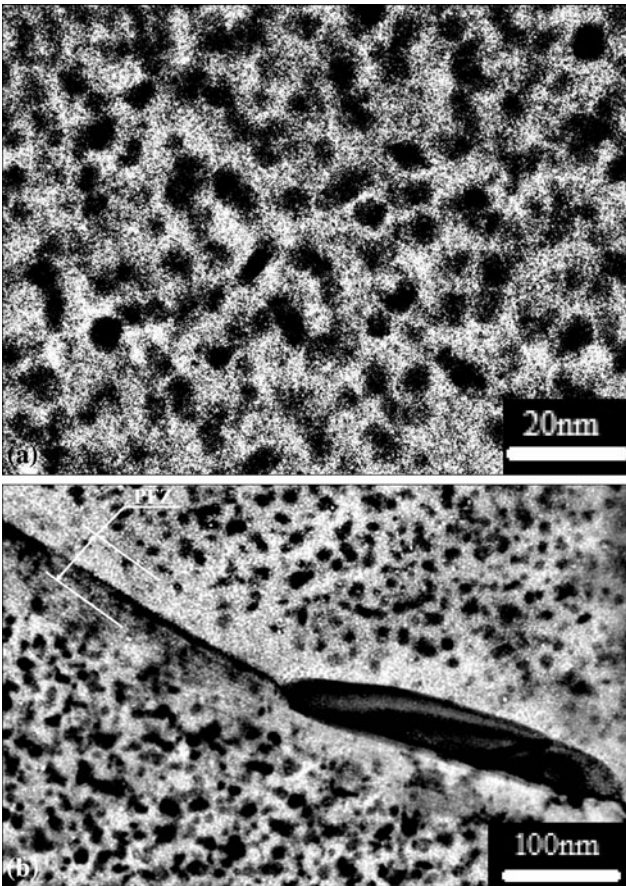


**Fig. 12** (a) TEM image of AA7003/ER5356 grain matrix after T73 heat treatment. (b) TEM image of AA7003/ER5356 grain boundary after T73 heat treatment

after postwelding heat treatment, which is not observed in alloys welded with filler metals ER5183 and ER5556. This indicates that the ER5356 is the most suitable filler for welding Al-Zn-Mg alloys.

2. Postwelding T6 heat treatment applied to AA7003 and AA7005 welded with filler metal ER5356 can enhance precipitation hardening in the fusion zone. On the other hand, postwelding T73 heat treatment applied to AA7003/ER5356 and AA7005/ER5356 weldments, besides achieving fusion zone hardness enhancement, yields a wider PFZ on the grain boundary. Hence, postwelding

T73 heat treatment is a better approach to increasing fusion zone strength in weldments.

3. Appropriate choice of filler metal and heat treatment can enhance the overall mechanical strength of the welded AA7003 and AA7005 alloys.

## References

1. G. Fu, F. Tian, and H. Wang, Studies on Softening of Heat-Affected Zone of Pulsed-Current GMA Welded Al-Zn-Mg Alloy, *J. Mater. Process. Technol.*, 2006, **180**, p 216–220
2. T. Ma and G.D. Ouden, Softening Behaviour of Al-Zn-Mg Alloys due to Welding, *Mater. Sci. Eng. A*, 1999, **266**, p 198–204
3. W.H. Cubberly, *ASM Handbook*, Vol 6, American Society for Metal, 1993, p 528–536, 722–739
4. B. Hu and I.M. Richardson, Microstructure and Mechanical Properties of AA7075(T6) Hybrid Laser/GMA Welds, *Mater. Sci. Eng. A*, 2007, **459**, p 94–100
5. W. Gruhl, The Stress-Corrosion Behavior of High-Strength Al-Zn-Mg Alloys, *Aluminum*, 1978, **54**, p 323–325
6. F.M. Mazzolani, *Aluminum Alloy Structure*, 2nd ed., E & FN Spon, an imprint of Chapman & Hall, London, UK, 1995, p 7–8
7. W.R. Oates, *Welding Handbook*, Vol 3, American Welding Society, 1987, 26p
8. The Aluminum Association, Inc., International Alloy Designations and Chemical Composition Limits for Wrought Aluminum and Wrought Aluminum Alloys, Arlington, VA, 2009, p 14
9. E.L. Rooy, *Metals Handbook, Properties and Selection: Nonferrous Alloys and Pure Metals*, 10th ed., Vol 2, ASM, 1986, p 124–131
10. M.O. Speidel, Stress Corrosion Cracking of Aluminum Alloys, *Metall. Trans. A*, 1975, **6A**, p 631–642
11. S. Kou and Y. Le, Grain Structure and Solidification Cracking in Oscillated Arc Welds of 5052 Aluminum Alloy, *Metall. Trans.*, 1985, **16A**, p 1345–1352
12. J.D. Embury and B. Nicholson, The Nucleation of Precipitates: The System Al-Zn-Mg, *Acta Metall.*, 1965, **13**, p 403–417
13. G.E. Metzger, Some Mechanical Properties of Welds in 6061 Aluminum Alloy Sheet, *Weld. J.*, 1967, **56**(10), p 457–469
14. G.W. Lorimer and B. Nicholson, Further Results on the Nucleation of Precipitates in the Al-Zn-Mg System, *Acta Metall.*, 1966, **14**, p 1009–1013
15. T. Ogura, S. Hirose, and T. Sato, Quantitative Characterization of Precipitate Free Zones in Al-Zn-Mg(-Ag) Alloys by Microchemical Analysis and Nanoindentation Measurement, *Sci. Technol. Adv. Mater.*, 2004, **5**, p 491–496
16. S.R. Yeomans, *Mechanical Property Variations Across Welded Joints in Aluminium Alloy 5083 and the Effects of Postweld Cold Working*, Research Report no. R-37, The University of New South Wales, 1988, p 1–21
17. J.J. Thompson, E.S. Tankins, and V.S. Agarwala, A Heat Treatment for Reducing Corrosion and Stress Corrosion Cracking Susceptibilities in 7xxx Aluminum Alloys, *Mater. Perform.*, 1987, **26**, p 45–52
18. J.C. Werenskiold, A. Deschamps, and Y. Bréchet, Characterization and Modeling of Precipitation Kinetics in an Al-Zn-Mg Alloy, *Mater. Sci. Eng. A*, 2000, **293**(1–2), p 267–274